Int. J. Heat Mass Transfer. Vol. 20, pp. 927–934. Pergamon Press 1977. Printed in Great Britain

EQUILIBRIUM HEAT AND MASS TRANSFER IN REGENERATORS IN WHICH CONDENSATION OCCURS

J. G. VAN LEERSUM*
Department of Mechanical Engineering, University of Western Australia, Nedlands, Western Australia, Australia

and

P. J. BANKS
Division of Mechanical Engineering, Commonwealth Scientific and Industrial Research Organization, Highett, Victoria, Australia

(*Received* 29 *December* 1975 *and in revised form* 19 *November* 1976)

Abstract—The processes which occur when air blows through a non-sorbing matrix with conditions such that water condenses on it are described using a theoretical model in which air, matrix and condensed water are in thermodynamic equilibrium at any location. Seven different types of waves are found to occur. The equilibrium model is used to predict the wave patterns and heat- and moisture-transfer effectivities for a balanced and symmetric regenerator with a non-sorbing matrix under conditions when condensation occurs. The wave pattern is found to become more complex and effectivities to increase as the cycle time of the regenerator decreases. The maximum obtainable total heat (enthalpy) effectivity is greater when condensation occurs, than when heat transfer only takes place in the regenerator. This is because the moisture transfer is non zero in the former case.

NOMENCLATURE

C_r, regenerator capacity rate ratio, see equation (9) [dimensionless];
h, air enthalpy [kJ/kg dry air];
H, matrix enthalpy [kJ/kg dry matrix];
L, length of matrix [m];
P, concentration of dry matrix mass per unit volume excluding interstices [kg/m^3];
t, air and matrix temperatures [°C];
v, air velocity through matrix interstices [m/s];
V, velocity of a sharp fronted wave [m/s];
w, air–water content [kg water/kg dry air];
W, matrix–water content [kg water/kg dry matrix];
x, distance into matrix in air flow direction [m].

Greek symbols

α_a, $-\left(\frac{\partial t}{\partial w}\right)_a$, slope of an adiabatic saturation line [°C];
α_s, $-\left(\frac{\partial t}{\partial w}\right)_s$, slope of the saturation line [°C];
γ, defined in equation (4) [dimensionless];
$\bar{\gamma}$, mean value of γ [dimensionless];
ε, interstitial volume of matrix per unit total volume [dimensionless];
η_h, enthalpy effectivity [time averaged outlet air enthalpy for one period—corresponding inlet air enthalpy]/[difference between two relevant inlet air enthalpies] [dimensionless];
η_t, temperature effectivity, same as η_h except temperature replaces enthalpy;
η_w, moisture effectivity, same as η_h except water content replaces enthalpy;
θ, time from beginning of a regenerator period [s];
θ_p, time for one regenerator cycle [s];
μ, $P(1-\varepsilon)/\rho\varepsilon$ [dimensionless];
ρ, air density [kg/m^3];
σ, specific heat ratio: matrix to air [dimensionless].

Subscripts

A (or B etc.), at or in thermodynamic equilibrium with state A (or B etc.); dry, matrix at this state has no water in it; wet, matrix at this state has a positive amount of water on it.

INTRODUCTION

THE PERFORMANCE of heat and mass regenerators has been discussed by Maclaine-Cross and Banks [1]. The theory presented there is only applicable when the matrix is sorbing without a discontinuity in matrix sorbate content along the sorption isotherm. That is, in the case of a regenerator with a non-sorbing matrix, it is assumed that no condensate forms on the matrix, hence only sensible heat is transferred. Although this assumption is adequate for such a regenerator used for heat recovery in the majority of air-conditioning applications, there do exist situations where, by virtue of the required indoor air state, and the actual outdoor state, condensation occurs during some part of the regenerator cycle. This paper shows that a similar

*Formerly Department of Mechanical Engineering, Monash University, Clayton, Victoria, Australia.

approach to that in [1] may be used to analyse the operation of such a regenerator. Infinite heat-transfer coefficients between the matrix and the air flowing over it are assumed. These, together with the Lewis relation, immediately imply infinite mass-transfer coefficients between air and matrix. Although this is a considerable idealization, it is felt that valuable insight into the mode of operation of such a regenerator may be gained by using this assumption.

Hausen [2] has considered the problem of condensation in regenerators and, for an equilibrium model, derived equations equivalent to (1) and (2). He presented graphical methods of solution based on finite difference techniques. All of his methods are approximate, and the only results given apply to extremely low temperature applications of the regenerator. Though his methods are applicable, in principle, to the present problem, their implementation, would be very tedious without using a digital computer. However, if the latter were used, the obtained results would be necessarily approximations, not as accurate as those obtained by the following method. This is exact, within the confines of a few minor assumptions. For this reason, no comparison of Hausen's with the present method has been made, except in so far as to note that in some ways, Hausen's methods are, in fact, approximations of the method described in this paper.

Attention is confined to regenerators where equal mass flow rates of the same fluid flow through equal facial areas in each period. The following analysis applies to both counterflow rotary and counterflow switched bed regenerators. The material in this paper is an expansion of van Leersum and Banks [3], and as such, supercedes the latter.

1. THE TYPES OF WAVES OCCURRING IN A REGENERATOR WITH A NON-SORBING MATRIX OPERATING WITH CONDENSATION

1.1. *The conservation equations*

The regenerator matrix consists of many parallel plates spaced equal distances apart. Air flows through these spaces in one direction, transferring heat and moisture to or from the matrix.

It is assumed that any moisture condensing on the matrix remains, not being drained away or blown off by the airflow. Evaporation occurs by some combination of the heat- and mass-transfer mechanisms described in Section 1.3, Section 1.4 and Section 1.6. For a regenerator operating in the steady state, there is no nett accumulation of condensate on the matrix, because the amount of moisture condensed per cycle must be equal to that evaporated in the same cycle. Numerical estimates of the amount of moisture condensed on the matrix are given in Section 2.3, and for a thin matrix material their magnitudes are in accord with the supposition that condensation is in the form of droplets. During qualitative experiments, using a matrix of parallel glass plates stacked vertically, condensation in the form of a fog was observed, and no self drainage was detectable, the fog evaporating as the matrix temperature approached that of the inlet air. That is, surface tension forces appear capable of holding the condensate to the plates.

The equations describing conservation of energy and moisture are, as in Banks [4]:

$$\frac{\partial w}{\partial \theta}+v\frac{\partial w}{\partial x}+\mu\frac{\partial W}{\partial \theta}=0 \tag{1}$$

$$\frac{\partial h}{\partial \theta}+v\frac{\partial h}{\partial x}+\mu\frac{\partial H}{\partial \theta}=0 \tag{2}$$

where the symbols are defined in the nomenclature list. The assumption of infinite transfer coefficients means that the matrix and any condensed water are in thermodynamic equilibrium with the air at any point.

Before considering the regenerator, the case of a matrix at uniform state exposed to a step change in inlet air state from equilibrium will be considered.

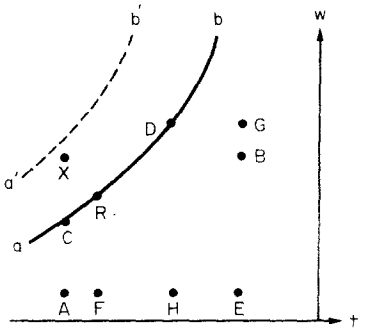

FIG. 1. A psychometric chart showing the relative positions of states *A*, *C*, *F*, *R*, *H*, *E*, *D*, *G* and *B* if *a*–*b* represents the air–water vapour saturation line, and the relative positions of states *A*, *X* and *B* if *a'*–*b'* represents the saturation line.

With reference to Fig. 1, if line *a'*–*b'* represents the saturation line, and air at state *B* is blown over a matrix, initially in equilibrium with air at state *A*, then it follows from [4] that the matrix will experience two distinct waves. The first of these will move at the fluid velocity, bringing the matrix to equilibrium with air at state *X* and the second will move at the velocity, $v/(1+\mu\sigma)$, since it is a heat-transfer wave moving through the bed taking the matrix formerly in equilibrium with air at state *X*, to equilibrium with air at state *B*. Under the assumption of constant specific heat ratio, the second front is sharp fronted as well as the first.

1.2. *The Flv wave*

If the saturation line in Fig. 1 is represented by the line *a*-*b*, the dew point temperature of state *B* is greater than the dry bulb temperature at state *A* and heat transfer only, as described in Section 1.1 does not occur. Instead, condensation must form on the matrix. Before this can happen, the matrix must move into equilibrium with saturated air. Because $\partial W/\partial\theta$ is initially zero, equation (1) becomes:

$$\frac{\partial w}{\partial \theta}+v\frac{\partial w}{\partial x}=0.$$

This equation is merely a kinematic wave equation

for a step change in w propagating through the matrix with velocity v. A step change in w of magnitude $w_C - w_A$ thus occurs before the matrix starts wetting, that is, the system first experiences a wave which takes its state from A to C. This wave will henceforth be referred to as the Flv wave.

1.3. *The condensation (Cnd) and evaporation (Evp) waves*

Once the system is in equilibrium with air at state C, $\partial W/\partial\theta$ is no longer zero, and moisture begins to form on the matrix: Since the air in equilibrium with the matrix must now be saturated, the system state must 'move up' the saturation line, where t is an explicit function of w and hence h can be expressed as a function of either t or w. Equation (2) can then be expressed solely in terms of w and W, since H can also be written in terms of w and W. Therefore equations (1) and (2) can be reduced to the form:

$$\frac{\partial w}{\partial\theta} + \frac{v}{(1+\mu\gamma)}\frac{\partial w}{\partial x} = 0 \tag{3}$$

where

$$\gamma = \sigma \Big/ \left(1 - \frac{\alpha_a}{\alpha_s}\right) \tag{4}$$

with α_a and α_s being the slopes on a psychrometric chart of the adiabatic saturation line and the saturation line at a given system state. This is just the result obtained by Banks [4] for the case of a matrix with infinite sorbability for water vapour in saturated air. By definition of α_a and α_s (Nomenclature), $\alpha_a/\alpha_s < 0$, so that $\gamma < \sigma$. Moving up the saturation line in the direction of increasing temperature, increases σ slightly, and decreases α_s in magnitude, α_a remaining closely constant. The nett effect of this is to make γ decrease with an increase in w. It can be shown from equations (1) and (3) that:

$$\gamma\frac{\partial w}{\partial\theta} = \frac{\partial W}{\partial\theta}. \tag{5}$$

The form of equation (3) is that of a kinematic wave changing the value of the quantity, w, with velocity $v/(1+\mu\gamma)$. Because of the functional variation of $v/(1+\mu\gamma)$ with w, an initial step change in w would tend to propagate with the leading edge propagating slower than the trailing edge. Such a situation is physically impossible as it implies that at any one time, each point in the region of the matrix near the wave front takes on three different values of w simultaneously. In reality, a sharp fronted wave, analogous to a shock wave, propagates through the matrix depositing water.

All segments of this wave front move with the same velocity:

$$v/(1+\mu\bar{\gamma}),$$

where $\bar{\gamma}$ is a mean value of γ evaluated over the relevant saturation line operating range. If an operating range less than 20°C is used, there is little inaccuracy incurred by linearizing this curve [5]. In the remainder of this paper, a linearized saturation line slope, α_s, will be assumed. Equation (3) with $\gamma = \bar{\gamma}$ then describes a sharp fronted condensation (Cnd) wave, whilst equation (5) implies that:

$$\Delta W = \bar{\gamma}\Delta w.$$

If the matrix starts off wet, at a higher temperature than t_C (Fig. 1), and air at state C is blown over it, the above analysis still holds, except that since w is decreasing, γ increases, and rather than a shock type wave profile resulting, the wave front widens as it progresses. Since the saturation curve has been linearized for the purposes of this paper, the resulting evaporation (Evp) wave will be assumed to move with the same velocity as the Cnd wave, and be sharp fronted.

1.4. *The slow evaporation (Sep) wave*

Assuming that the passage of the Cnd wave leaves the matrix wet, in equilibrium with air at some state D (Fig. 1) on the saturation line, some final change must occur to bring the matrix to equilibrium with air at state B (Fig. 1). This necessitates the drying out of the matrix, i.e. an evaporation wave. The conservation equations (1) and (2) must still apply. For the special case of infinite transfer coefficients, it is concluded that the water must be removed from the matrix by a sharp fronted wave, that is, it can't be removed gradually since this would imply a matrix segment which was wet, but did not have the air state in equilibrium with it on the saturation line. This is clearly impossible. A sharp fronted wave must propagate through the matrix. This wave must simultaneously remove all water from the matrix and bring both air and matrix states to state B (Fig. 1). Banks [4] has shown that the condition for such a wave is:

$$\frac{\Delta H}{\Delta W} = \frac{\Delta h}{\Delta w} \tag{6}$$

so that

$$\frac{H_D - H_B}{W_D - W_B} = \frac{h_D - h_B}{w_D - w_B}$$

with $W_B = 0$ and $W_D = \bar{\gamma}(w_D - w_C)$ from Section 1.3. This wave will henceforth be referred to as the Sep wave.

The only unknown is point D on the saturation line, which can then be found from (6). Banks [4] also shows that the velocity of propagation of such a wave is:

$$V = v/(1+\mu\Delta W/\Delta w) \tag{7}$$

so that

$$V = v/[1+\mu\bar{\gamma}(w_D - w_C)/(w_D - w_B)].$$

This then completes the description of the processes which occur when air at state B blows over a matrix initially in equilibrium with air at state A, such that condensation and evaporation occur.

1.5. *The "wave diagram" for the Flv, Cnd and Sep waves*

The passage of the Flv, Cnd and Sep waves through a matrix of length L for a time θ_p can be conveniently represented on a wave diagram [1, 5] shown in Fig. 2.

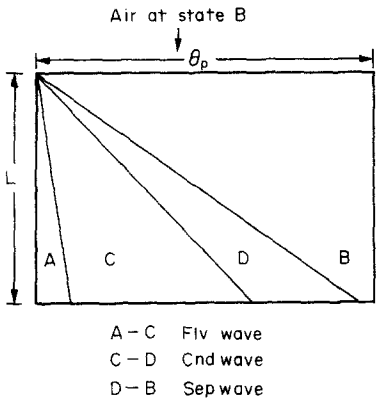

FIG. 2. A "wave diagram" for the waves which occur when air at state B (Fig. 1) blows over a matrix initially in equilibrium with air at state A (Fig. 1).

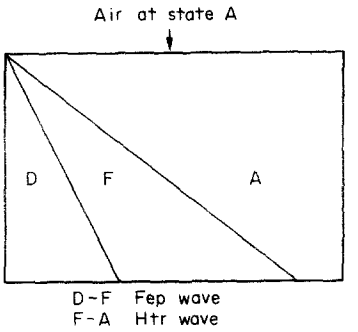

FIG. 3. A wave diagram showing the waves which occur when air at state A blows over a matrix initially wet, in equilibrium with air at state D, where $W_D < \bar{\gamma}(w_D - w_A)$. Relative positions of states A, D and F are shown in Fig. 1.

At any particular time, this wave diagram allows determination of matrix state variation with position in the matrix for an equilibrium model. In such a diagram, the ordinate is distance into the matrix in the air flow direction, whilst the abscissa is time. Each wave is represented by a line with slope equal to the wave velocity. The velocity of the Flv wave is v, clearly greater than $v/(1+\mu\bar{\gamma})$, the Cnd wave velocity, approximately the same as the Evp velocity. The Sep wave velocity, $v/[1+\mu\bar{\gamma}(w_D-w_C)/(w_D-w_B)]$, is less than the Cnd wave velocity, because $(w_D-w_C)/(w_D-w_B) \geqslant 1$. Hence the wave diagram appears as in Fig. 2, with regions bounded by lines of different slope being at constant states, marked in the figure.

1.6. *The fast evaporation (Fep) wave*

If a matrix is initially wet, in equilibrium with air at some state D, and a drying air stream at state A (Fig. 1) is blown over the matrix, it must ultimately dry out. It may be shown [5, 6], that provided $W_D < \bar{\gamma}(w_D - w_A)$, a sharp fronted wave, termed the Fep wave, takes the system into equilibrium with some state F (Fig. 1) such that:

$$\frac{H_D - H_F}{h_D - h_F} = \frac{W_D - W_F}{w_D - w_F} \tag{8}$$

with

$$W_F = 0 \text{ and } w_F = w_A.$$

The velocity of this wave is:

$$v/[1+\mu W_D/(w_D - w_A)].$$

If, for example, $W_D = \bar{\gamma}(w_D - w_C)$ (Fig. 1) and inlet air at state A were blown through the system, an Fep wave would occur. Following this, a heat-transfer (Htr) wave, as described in Section 1.1 takes the system to final equilibrium with air at state A. Figure 3 represents the wave diagram for such a system.

Note that $W_D = \bar{\gamma}(w_D - w_C)$, and because $(w_D - w_C)/(w_D - w_A) < 1$, the Fep wave is faster than the Cnd wave. The heat-transfer wave velocity, $v/(1+\mu\sigma)$, is less than the Cnd wave velocity, because σ is greater than γ [equation (4)], hence the velocity of the heat transfer only wave is also less than the velocity of the Fep wave.

For a regenerator operating in the steady state, the maximum amount of moisture on the matrix is less than $\bar{\gamma}(w_D - w_A)$ for all wet matrix states, D, and drying air states, A, thus no further theory on drying waves will be advanced. In another paper [6], the drying processes which occur when a matrix initially in equilibrium with air at state D and with $W_D > \bar{\gamma}(w_D - w_A)$, is subjected to inlet air at state A are discussed.

1.7. *The stationary (Sta) wave*

This wave occurs as a result of having the upstream part of the matrix in equilibrium with air at state D (Fig. 1) and wet as well, together with the rest of it in equilibrium with air at state B. Suppose air at state A then blows over the matrix as in Fig. 4(I). The assump-

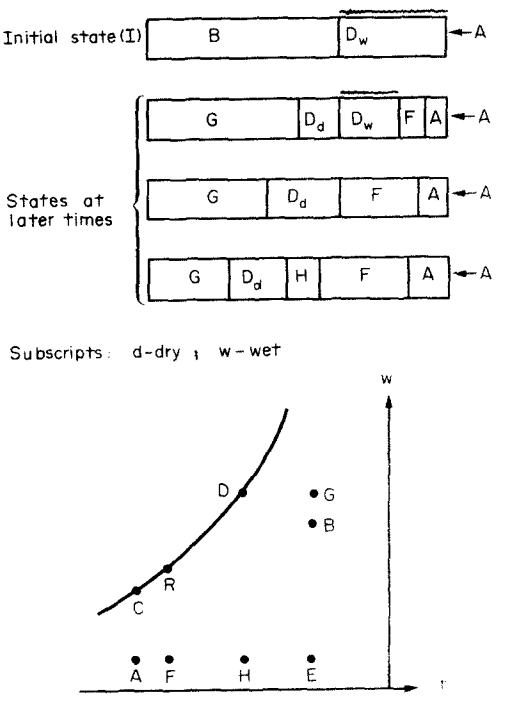

FIG. 4. (Top) A diagram showing the four main transitions that a matrix, initially partially wet as shown in (I) goes through when air at state A enters the matrix as shown in (I). (Bottom) A psychometric chart showing the relative positions of all states referred to in the top figure.

tions of infinite transfer coefficients imply that the matrix states immediately bring the air above them to equilibrium, hence at the discontinuity between states B and D, the matrix at B receives saturated air at state D. Banks [4] implies that a sharp fronted Flv wave moves through the B part of the matrix, taking it into equilibrium with air at state G (Fig. 4), followed by a slower heat-transfer wave shifting the matrix state from G to D_{dry}, that is, to be dry in equilibrium with air at state D. There thus exists a state D_{dry}, adjacent to state D_{wet} (Fig. 4). From (7), the velocity of the front between the two states is:

$$v/[1+\mu(W_{D_{wet}}-W_{D_{dry}})/(w_{D_{wet}}-w_{D_{dry}})] = 0$$

since $w_{D_{dry}} = w_{D_{wet}}$, indicating that the front remains stationary.

Initially, at the front of the matrix, air at state A strikes a wet matrix in equilibrium with air at state D, initiating an Fep wave (Section 1.6). The Fep wave propagates into the matrix until the wet part of the matrix is dry. Only then do the Fep and Sta waves cease to propagate, and the system comes to equilibrium as shown in the last two matrix state diagrams in Fig. 4. Figure 5 is a wave diagram of the entire process.

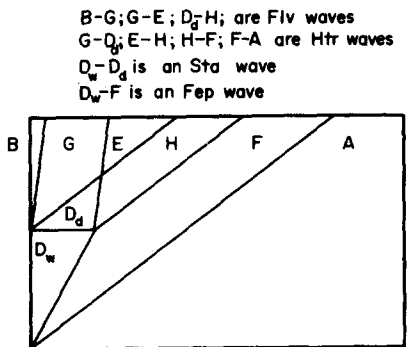

FIG. 5. The wave diagram corresponding to the situation described in Fig. 4.

1.8. *The wave velocities*

Seven waves have been discussed and represented on wave diagrams. In [5], it is shown that the Htr wave velocity is greater than the Sep wave velocity. This, together with the remarks made about the relative magnitudes of other wave velocities in Section 1.5, implies that:

> Flv wave velocity = v > Fep wave velocity > Cnd wave velocity ≃ Evp wave velocity > Htr wave velocity > Sep wave velocity > Sta wave velocity = 0.

It can also be shown [5] that D lies below the intersection of the wet bulb line through B and the saturation line.

2. THE REGENERATOR

In a regenerator, the boundary conditions can be represented on a wave diagram as in Fig. 6. The most important rule which must be obeyed in these diagrams

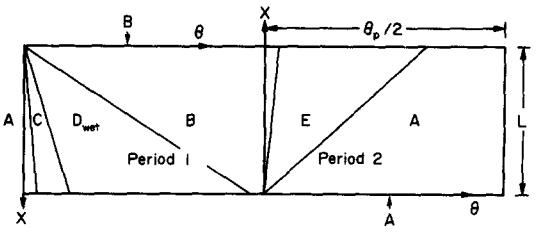

FIG. 6. The simplest regenerator wave diagram corresponding to inlet states A and B. Relative positions of all states are shown in Fig. 1.

is the reversal condition. Period one is repeated after period two, so that the two ends (left and right) of the wave diagram are physically the same. Therefore waves starting at the left hand edge must, in position but not gradient, exactly match those finishing at the right hand edge. A similar condition must be obeyed at the centre of the wave diagram, that is the end of period one and the beginning of period two. To obtain effectivities, the relevant quantity must be time averaged at the outlet state; this is easily accomplished since time is the horizontal axis. So far as can be seen, the seven different types of waves mentioned in section one are the only ones which occur in the regenerator considered. Thus all the wave diagrams discussed later are composed of various combinations of these seven waves. The parameter determining regenerator performance, which depends on the regenerator period time, is the capacity rate ratio, defined by

$$C_r = 2L(1+\mu\sigma)/v\theta_p \qquad (9)$$

where L is the length of the regenerator matrix in the air flow direction, and $v/(1+\mu\sigma)$ is the Htr wave velocity. For the rotary regenerator considered, θ_p is the time for one revolution of the matrix. C_r is really the dimensionless time for an Htr wave to pass through the regenerator, and is used here as a measure of the regenerator's rotational speed.

2.1. *Example 1*

The simplest type of wave diagram occurs for heat transfer only and is fully discussed in [1]. In the case of condensation, the simplest wave diagram is shown in Fig. 6. A and B (Fig. 1) are the two inlet states and D is obtained from Section 1.4. The rest of the states are shown in Fig. 1. Waves A–C and B–E are Flv waves and extremely fast compared with waves C–D_{wet} (Cnd), D_{wet}–B (Sep), and E–A (Htr). The slopes of the Flv waves are enlarged in Fig. 6 and other wave diagrams, to make them recognisable. In this example there is no difficulty in meeting the reversal condition because all waves reach the end of the regenerator before the period time is expired.

2.2. *Example 2*

The previous example applies only for a very slow regenerator rotational speed. At such speeds, the heat and moisture effectivities are very low, hence the whole process is of academic interest only. The next step in complexity involves the wave diagram shown in Fig. 7.

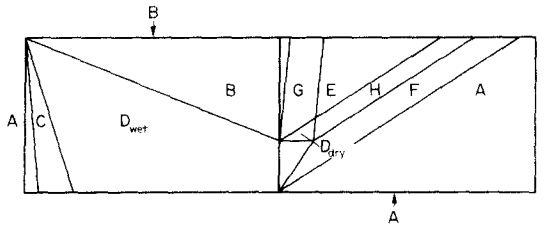

FIG. 7. The regenerator wave diagram when the D_{wet}–B (Sep) wave does not propagate completely through the matrix in period 1.

This shows just how complicated the diagram can become for a small increase in speed. The added waves occur simply because the D_{wet}–B wave does not completely travel through the matrix in period one. A–C, B–G, G–E, D_{dry}–H, are Flv waves, C–D_{wet} is a Cnd wave, D_{wet}–B is a Sep wave, D_{wet}–D_{dry} is an Sta wave, D_{wet}–F is an Fep wave whilst G–D_{dry}, E–H, H–F and F–A are Htr waves. State D is as in example 2.1 and state F can be found from Section 1.6.

The RHS of the wave diagram is identical to Fig. 5.

2.3. *A more complicated numerical example*

Figure 8(a) is a scale wave diagram corresponding to a regenerator running at a C_r value of 1.52 between the inlet conditions A, B [Fig. 8(c)]. To emphasize the meaning of such a diagram, the actual matrix states at various times are shown in Fig. 8(b). All matrix states except the following are dry.

State	Amount of water on matrix (kg water/kg dry matrix)
D_{wet}	$\bar{\gamma}(w_D - w_C) = 0.00185$
$R(1)$	$\bar{\gamma}(w_R - w_C) = 0.00034$
$S(1)$	$\bar{\gamma}(w_S - w_C) = 0.00179$
S	$\bar{\gamma}(w_S - w_R) = 0.00145$

Figure 8(c) shows the actual positions of all states. States $R(1)$ and $S(1)$ are identical to states R and S respectively, except for their W values. The concentration of water at these states is given above.

$\bar{\gamma}$ was obtained from Section 1.3 assuming the constant saturation line slope shown in Fig. 8(c).

State D is calculated from equation (6) with $W_B = 0$ and $W_D = \bar{\gamma}(w_D - w_C)$.

State F is calculated from equation (6) applied between states D and F with $W_F = 0$ and $w_F = w_A$.

State S is calculated from equation (6) applied between states S and B with $W_B = 0$ and $W_S = \bar{\gamma}(w_S - w_R)$ where $t_R = t_F$ and R is on the saturation line

F–R, A–C, B–G, G–E, D_{dry}–H are Flv waves.

R–S, C–$R(1)$, $R(1)$–$S(1)$, $S(1)$–D_{wet} are Cnd waves.

S–B, D_{wet}–B are Sep waves.

S–$S(1)$, R–$R(1)$, D_{dry}–D_{wet} are Sta waves.

D_{wet}–F is an Fep wave.

E–H, H–F, F–A, G–D_{dry} are Htr waves.

By time averaging the outlet states, the effectivities were found to be:

$$\eta_h = 0.31 \quad \eta_w = 0.12 \quad \eta_t = 0.76$$

assuming the matrix to be constructed from mylar film giving $\mu\sigma = 114$. Since the air properties were linearized, the values of η_t for both periods were equal.

3. REALISTIC EXAMPLE

Regenerator inlet conditions were chosen to realistically approximate those which might occur in Darwin, Australia. They were:

indoor conditions (desired) 21.1°C dry bulb, 55% r.h., [Point A on Fig. 8(c)]
outdoor conditions (typical) 34.4°C dry bulb, 60% r.h., [Point B on Fig. 8(c)].

The regenerator was considered to run at capacity rate ratio values of 1, 1.52, 1.9, 2.9 and 3.8 and wave diagrams were drawn from the equilibrium theory presented above. The various resulting effectivities are shown in Table 1. The regenerator was assumed to have $\mu\sigma = 114$.

Table 1

C_r	Moisture effectivity	Temperature effectivity	Enthalpy effectivity
1.00	0.05	0.72	0.26
1.52	0.12	0.76	0.31
1.90	0.17	0.78	0.36
2.90	0.26	0.84	0.47
3.80	0.34	0.92	0.52

4. CONCLUSIONS

It can be seen that for each wave diagram drawn, the matrix, and hence fluid mean outlet states of period 1 are all at nearly saturated conditions. This is because all but one of the different outlet states occuring during period 1 lie on the saturation line. The exception is the state, A, which persists as an outlet state until the Flv wave reaches the regenerator outlet, changing state A to C (Fig. 1). Since this wave is extremely fast compared with the other waves, the outlet state of the regenerator segment is at A only for a very short time, in comparison with the time it is at the other saturated outlet states. Only when the regenerator is run at a very high rotational speed, so that the Flv wave takes a significant proportion of the period length to pass through the regenerator, is the latter statement untrue. At this stage, a large proportion of the air entering the regenerator, is carried over physically from one period to the next, so that the regenerator acts as a positive displacement pump, instead of a heat exchanger. To avoid this, the regenerator should always be run so that the blow through time of the Flv wave is less than 5% of the period length, implying that for the above examples,

$$\frac{2L}{v\theta_p} < 0.05 \text{ or } C_r = \frac{2L}{v\theta_p}(1 + \mu\sigma) < 5.75.$$

This ensures that "carryover" is small, and the mean outlet state of period 1 is virtually saturated, except for very low values of C_r when all waves blow through the matrix before period 1 ends.

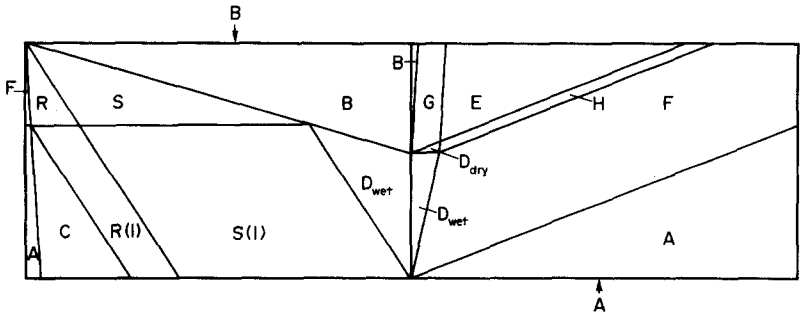

FIG. 8(a). A wave diagram corresponding to the practical situation of Section 2.3. $C_r = 1.52$ and $\mu\sigma = 114$. Figure 8(c) shows the matrix and air inlet states on a scale drawing of a psychrometric chart.

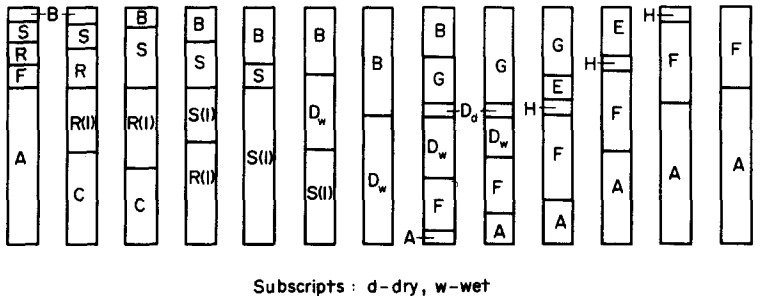

FIG. 8(b). Diagrammatic representation of matrix from the wave diagram in Fig. 8(a), depicting at various times, the proportion of matrix segment at the shown states.

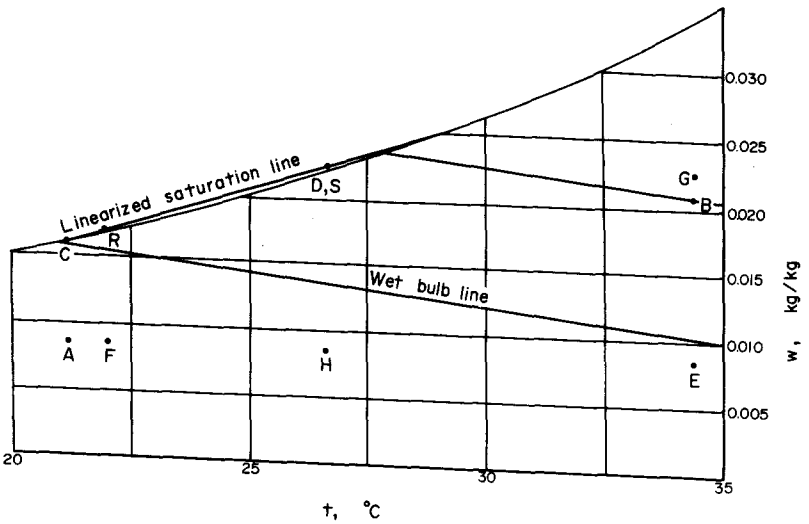

FIG. 8(c). A psychrometric chart showing the states referred to in Figs. 8(a) and (b).

Table 1 shows that effectivities increase with increasing dimensionless speed. Because the mean air outlet state of period 1 is always saturated, it moves down the saturation line toward C, as dimensionless speed is increased. Since the mean outlet state of period 1 must always be saturated, to avoid carryover, C appears to be the limiting mean outlet state of period 1. That is, the maximum total heat (enthalpy) effectivity obtainable in a regenerator where condensation occurs is $(h_B - h_C)/(h_B - h_A)$. For the realistic example given above, the maximum enthalpy effectivity obtainable with a purely sensible heat regenerator, if the saturation line were positioned where no condensation could occur, would be 0.25. Table 1 shows enthalpy effectivities far in excess of this value, when condensation occurs. Furthermore, if the mean outlet state of period 1 is state C, enthalpy effectivity rises to 0.59. For $C = 3.8$, enthalpy effectivity is 0.52 (Table 1), so C appears to be a feasible limiting mean outlet air state for period 1, as discussed above.

In practical situations, all heat- and mass-transfer coefficients are finite, and therefore a non-equilibrium model of the regenerator is necessary. Such a model has been constructed, using a digital computer simulation of the regenerator. Detailed results using this model, together with a comparison between results for

finite and infinite heat- and mass-transfer coefficients are given in van Leersum [7]. Suffice it to say that for practical cases, effectivities seem to be about 75% of equilibrium model effectivities, all other parameters being equal. Unfortunately, the non equilibrium model is not developed in terms of non dimensional inlet states, so each pair of inlet states has to be fed into the model when required. Only a small number of cases have therefore been checked, and the above conclusion regarding the non equilibrium model in comparison with the equilibrium model was drawn from this limited number of results. It was certainly true that as transfer coefficients were increased to about 10 times their value in a normal situation, effectivities predicted by the non equilibrium model approached those from the equilibrium model described in this paper.

Wave diagrams as applied to the equilibrium model can thus serve as a check on a non equilibrium model as transfer coefficients are increased in value. The real value of these diagrams lies in the insight they can give to the types of processes which occur in a regenerator where condensation and evaporation take place. That is, wave diagrams are useful aids to understanding the way in which condensate forms and is removed from a regenerator matrix.

Initially, it was decided to produce a "wave diagram drawing" computer program. This idea was abandoned because for one set of inlet states, it was estimated that there could be over 100 different diagrams for C_r less than 5. Instead, attention was concentrated on producing a non equilibrium model of the regenerator operating with condensation and evaporation taking place [7].

Acknowledgement—The first author is grateful for the assistance of a Commonwealth Post Graduate Scholarship during the course of this work.

REFERENCES

1. I. L. Maclaine-Cross and P. J. Banks, Coupled heat and mass transfer in regenerators, prediction using an analogy with heat transfer, *Int. J. Heat Mass Transfer* **15**, 1225–1242 (1972).
2. H. Hausen, *Wärmeubertragung im Gegenstrom, Gleichstrom und Kreuzstrom*. Springer, Berlin (1950).
3. J. G. van Leersum and P. J. Banks, Heat and mass transfer in regenerators in which condensation occurs. 1st Australasian Conference on Heat and Mass Transfer, Section 5.4; pp. 1–8, Melbourne (1973).
4. P. J. Banks, Coupled equilibrium heat and single adsorbate transfer in fluid flow through a porous medium—1. Characteristic potentials and specific capacity ratios, *Chem. Engng Sci.* **27**, 1143–1155 (1972).
5. J. G. van Leersum, Heat and mass transfer in regenerators, Ph.D. Thesis, Department of Mechanical Engineering, Monash University (1975).
6. P. J. Banks and J. G. van Leersum, The temperature of drying, Paper in preparation.
7. J. G. van Leersum, Heat and mass transfer in regenerators in which condensation occurs: a non-equilibrium model, Paper in preparation.

TRANSFERT DE MASSE ET DE CHALEUR DANS LES REGENERATEURS AVEC CONDENSATION

Résumé—On décrit les processus qui s'établissent quand l'air passe à travers une matrice sans sorption, dans des conditions telles que l'eau se condense sur elle. On utilise un modèle théorique dans lequel l'air, la matrice et l'eau condensée sont en équilibre thermodynamique en tout point. On trouve sept types d'ondes. Le modèle d'équilibre est utilisé pour prédire les configurations d'ondes et l'efficacité des transferts de chaleur et d'humidité, dans les conditions de condensation, avec une matrice sans sorption d'un régénérateur symétrique et équilibré. On trouve que la configuration d'onde devient plus complexe et que les efficacités augmentent quand la période du cycle du régénérateur décroît. L'efficacité maximale possible de chaleur totale (enthalpie) est plus grande avec condensation que lorsqu'il y a uniquement un transfert de chaleur. Ceci est dû au transfert non nul par l'humidité.

WÄRME- UND STOFFÜBERGANG IN REGENERATOREN MIT KONDENSATAUSFALL UNTER GLEICHGEWICHTSBEDINGUNGEN

Zusammenfassung—Die Vorgänge, die beim Durchströmen einer nicht-sorptiven Matrix mit feuchter Luft bei gleichzeitigem Kondensatausfall auftreten, werden unter Verwendung eines theoretischen Modells, in dem Luft, Matrix und auskondensiertes Wasser an jeder Stelle in thermodynamischem Gleichgewicht, sind, beschrieben. Es wurde festgestellt, daß sieben verschiedene Wellenformationen auftreten. Das Gleichgewichtsmodell wird zur Vorausbestimmung der Wellenart und des Wärme- und Feuchtigkeitstransports in einem ausgeglichenen und symmetrischen Regenerator mit nicht-absorbierender Matrix und Kondensatausfall verwendet. Mit abnehmender Periodenzeitdauer wird das Wellenmuster komplexer und die Austauschraten größer. Die max. mögliche Wärmespeicherung ist bei Kondensatausfall größer als bei reinem Austausch fühlbarer Wärme, was auf den Feuchtigkeitstransport zurückzuführen ist.

ТЕПЛО- И МАССОПЕРЕНОС ПРИ ТЕРМОДИНАМИЧЕСКОМ РАВНОВЕСИИ В РЕГЕНЕРАТОРАХ С КОНДЕНСАЦИЕЙ

Аннотация — Описываются процессы, происходящие при продувании воздуха через сорбирующую матрицу при конденсации на ней воды. Для описания используется теоретическая модель, в которой воздух, матрица и сконденсированная вода при любом расположении находятся в термодинамическом равновесии. Найдено, что имеют место семь различных видов волн. Равновесная модель используется для определения волновых картин и эффективности переноса тепла и влаги в сбалансированном и симметричном регенераторе с несорбирующей матрицей при наличии конденсации. Найдено, что при уменьшении длительности цикла регенератора волновая картина становится более сложной и эффективность переноса тепла и влаги возрастает. Максимально достигаемая энтальпия больше при наличии конденсации, чем тогда, когда происходит только перенос тепла в регенераторе. Это объясняется тем, что в первом случае перенос влаги не равен нулю.